1 Title 2 Dispersal of hippos into central Europe during the last glacial 3 4 5 **Authors** 6 7 Patrick Arnold^{1,16}, Doris Döppes², Federica Alberti^{1,15}, Andreas Füglistaler³, Susanne Lindauer⁴, Christian 8 Hoselmann⁵, Ronny Friedrich⁴, Irka Hajdas⁶, Marc Dickinson⁷, Frank Menger⁸, Johanna L. A. Paijmans^{9,10}, Love Dalén^{11,12,13}, Daniel Wegmann^{3,14}, Kirsty E. H. Penkman⁷, Axel Barlow¹⁰, Wilfried 9 Rosendahl^{2,4}, Michael Hofreiter¹ 10 11 12 13 Affiliations 14 ¹Evolutionary Adaptive Genomics, Institute of Biochemistry and Biology, University Potsdam, Karl-Liebknecht-Straße 24-25, 14476 Potsdam, Germany 15 16 ²Reiss-Engelhorn-Museen, Zeughaus, C5, 68159 Mannheim, Germany 17 ³Department of Biology, University of Fribourg, Chemin du Musée 15, 1700 Fribourg, Switzerland 18 ⁴Curt-Engelhorn-Zentrum Archäometrie gGmbH, C4/8, 68159 Mannheim, Germany 19 ⁵Hessisches Landesamt für Naturschutz, Umwelt und Geologie, Dezernat G1 Geologische Grundlagen, Rheingaustraße 186, 65203 Wiesbaden, Germany 20 21 ⁶Laboratory of Ion Beam Physics, ETH Zurich, Otto-Stern-Weg 5, 8093 Zurich, Switzerland 22 ⁷Department of Chemistry, University of York, York YO10 5DD, UK 23 8Hintergasse 21, 68649 Groß-Rohrheim, Germany 24 ⁹Department of Zoology, University of Cambridge, Downing Street, Cambridge, CB2 3EJ, United 25 Kingdom 26 ¹⁰Molecular Ecology and Evolution at Bangor, School of Natural Sciences, Bangor University, 27 Environment Centre Wales, Bangor LL57 2UW, Wales, United Kingdom 28 ¹¹Swedish Museum of Natural History, Department of Bioinformatics and Genetics, Box 50007, 10405 Stockholm, Sweden 29 ¹²Centre for Palaeogenetics, Svante Arrhenius väg 20c, 10691 Stockholm, Sweden 30 ¹³Department of Zoology, Stockholm University, 10691 Stockholm, Sweden 31

¹⁴Swiss Institute of Bioinformatics, 1700 Fribourg, Switzerland

33 34	Universitätsmedizin Berlin, Virchowweg 15, 10117 Berlin, German
35	¹⁶ Lead contact
36	
37	
38	Corresponding authors
39	Patrick Arnold: patrickarnold@uni-potsdam.de
40	Wilfried Rosendahl: wilfried.rosendahl@mannheim.de

Michael Hofreiter: michael.hofreiter@uni-potsdam.de

Summary

42

43

44 45

46 47

48

49

50

51

52

53

54

55

56

57

58

59

60

61

62

63

Late Pleistocene hippo fossils (Hippopotamus amphibius) from Europe have generally been associated with the last interglacial period (Eemian, 129 to 115 thousand years ago [ka])¹⁻⁴. As a widely-accepted indicator species for temperate climate conditions, it was assumed they went extinct with the onset of the last glacial (Weichselian) around 115 ka^{2,5}. Their origin and relationships to extant African common hippos and the exact age of their extinction in central Europe, however, remain unclear. We here address these questions using an integrated approach applied to hippos from the Upper Rhine Graben in central Europe. By sequencing the paleogenome of a European hippo, we reveal its close genetic links to modern hippos from Africa. Six additional partial mitochondrial genomes confirm that European representatives were part of the same, once widespread species that is today restricted to sub-Saharan Africa. Surprisingly, radiocarbon dating show that hippos were present in central Europe during the middle Weichselian (a period spanning from earlier than 47 ka until ~31 ka), i.e., well into the last glacial. Similar radiocarbon dates for woolly mammoth and woolly rhino fossils from the same sites imply short-term alternation of faunas during this period. Despite the paleogenome's low coverage, we are able to confidently estimate its genome-wide diversity by recalibrating the sequencing quality scores and assessing post-mortem damage. The low genome-wide diversity recovered suggests that it belonged to a small, isolated population. Overall, our combined data implies that hippos inhabited the Upper Rhine Graben refugium during temperate phases of the middle Weichselian.

64 Results and discussion

The Middle and Late Pleistocene of Europe was dominated by alternating glacial and interglacial periods⁶. A particularly exotic element of the European interglacial fauna were the hippopotami². Hippos colonized Europe from Africa in multiple waves, probably by multiple species of the genus Hippopotamus, including the common hippo (H. amphibius) that is today restricted to sub-Saharan Africa^{7–10}. During their maximal geographic distribution in Europe, hippos ranged from the British Isles in the northwest to the Iberian and Italian peninsula in the south8. Their presence in the fossil record generally implies temperate conditions with denser vegetation and open water bodies. Hence, it is a widely accepted indicator species for interglacial periods¹⁻⁴. Accordingly, it is generally assumed that both its peak prevalence and maximal geographic distribution in Late Pleistocene Europe coincides with the Eemian interglacial between 129 ka and 115 ka ago (corresponding to marine oxygen isotope stage (MIS) $5e^{2-4.8}$). The onset of cooling at the beginning of the subsequent last glaciation (Weichselian glaciation; 115 ka to 11.7 ka; corresponding to MIS 5d-2), consequently led to unfavorable conditions resulting in its extinction in western and central Europe^{2,5}. Their origin and relationships to extant African common hippos and the exact age of their extinction in central Europe, however, still remain unclear as, beyond morphological identification, only few detailed analyses have been performed on Late Pleistocene hippos, and ancient DNA data are notably absent for this species.

81

82

83

84

85

86 87

88

89

90 91

92

93

94

95

96

97

98

99

100

101

102

103

104

105

106

107

108

109

65 66

67

68

69

70

71

72 73

74

75

76 77

78

79

80

Close genetic links between Late Pleistocene European and extant African hippos

We subjected 19 hippo specimens from fossil localities in the Upper Rhine Graben in southwestern Germany to paleogenetic analysis (Figure 1A, Table S1). The Upper Rhine Graben represents the eastern-most boundary of Hippopotamus' Late Pleistocene distribution in central Europe^{3,8}. The long history of quarrying activities in the sandy-gravelly deposits (Mannheim formation¹¹, see STAR Methods for further details) unearthed numerous fossils of large mammal remains from the Late Pleistocene. As these deposits include representatives from both interglacial as well as glacial fauna, they have traditionally been interpreted as preserving the transition between the Eemian interglacial and the early Weichselian glacial (MIS4) in central Europe^{1-4,12-14}, and thus as evidence supporting the hypothesis that hippos went extinct at the end of the Eemian interglacial. Out of 19 analyzed samples, one (NK37 from the gravel pit Eich; Table S1) yielded a higher proportion of endogenous DNA and was sequenced to ~0.5x genomic coverage to elucidate phylogenetic relationships between Pleistocene European and extant African common hippos. Post-mortem damage patterns support the authenticity of ancient mapped reads (Figure S1). A Maximum Likelihood phylogenetic reconstruction, based on 3,085 concatenated 5kbp genomic windows sufficiently covered by paleogenetic data, places the Upper Rhine Graben hippo sample NK37 closer to the two extant African common hippos (ACH1, ACH2) than to the extant West African pygmy hippo (Choeropsis liberiensis), which was inferred as a distantly related outgroup (Figure 1B). However, the exact placement of NK37 in regard to the African common hippo specimens is unclear. The concatenated data set as well as 44% of window trees place NK37 as sister lineage to both ACH1 and ACH2 but 38% and 18% of window trees support a closer relationship of NK37 to ACH1 or ACH2, respectively (i.e., sample NK37 inside African common hippos, Figure 1B). This is further supported by D-statistics (Z = -5.77) that imply a closer relationship of sample NK37 to ACH1 than to ACH2. The discordance could stem from incomplete lineage sorting combined with phylogeographic structure in the ancestral African population. Alternatively, it could be the result of admixture between different hippo lineages in Africa or Europe.

Using enrichment by hybridization capture and stringent sequence calling methods, we additionally recovered partial mitogenomes for six Upper Rhine Graben specimens (completeness ranging from 15% to 78%; Table S1). Authenticity of ancient reads is again supported by post-mortem damage

patterns (Figure S1). Maximum Likelihood and Bayesian phylogenetic reconstructions suggest that Late Pleistocene hippos from the Upper Rhine Graben are closely related and form a monophyletic lineage that falls within the mitochondrial diversity of extant African common hippos (Figure 1C, Figure S2). An approximately unbiased test, however, cannot exclude (p = 0.131) a position outside extant African common hippos (similar to the main topology in the nuclear concatenation analysis above). Thus, the exact branching order at the beginning of the *H. amphibius* divergence cannot unambiguously be resolved. The close genetic link of Pleistocene hippos from the Upper Rhine Graben to extant African common hippos is also supported by haplotype networks based on a larger, continent-wide sample of mitochondrial cytB (854nt) and control region sequences¹⁵ (927nt; Figure S2). In all networks, Pleistocene hippos from the Upper Rhine Graben share haplotypes with specimens mostly known from eastern and south-eastern Africa. Mitochondrial distance among contemporary African common hippos from different regions in Africa is likewise larger than between Pleistocene hippos and some extant east African hippo lineages. These results show that these Late Pleistocene hippos from Europe do not form a divergent lineage but were part of the once widely-distributed common hippo that is now confined to sub-Saharan Africa.

125

126

127

128

129

130

131132

133

134

135

136

137

138

139

140141

142143

144

145

146

147

148

149

150

151

152

153

154

155

156

110

111

112

113

114

115

116117

118119

120

121

122

123

124

Middle Weichselian presence of hippos in central Europe

Given that their Eemian provenance is solely based on the assumption that hippos are indicative for interglacial conditions in Europe, we next evaluated the age of fossil specimens from the Upper Rhine Graben gravel pits by radiocarbon dating. Samples were collected from deeper layers within each bone to mitigate any bias due to the potential presence of conservatory chemicals that may have been used to treat the surface of fossil specimens for preservation (systematically tested previously¹⁶). Additionally, Fourier transform infra-red (FTIR) spectroscopy indicates that the collagen spectra closely resemble those of reference collagen, suggesting good preservation and purity (Figure S3). 28 out of 32 fossil hippo specimens selected for ¹⁴C analysis yielded enough collagen to be dated successfully. The analysis resulted in calibrated dates from the dating limit of ≥49 cal ka to as young as 31 cal ka (Figure 2, Table S2). Repeated dating for two samples (including in a second lab) confirmed their young age (Figure 2). Although exact calendar ages have to be interpreted carefully in this time period, our results suggest that hippos were - in contrast to previous assumptions - present in central Europe during MIS3, i.e. well into the middle of the last glacial period (middle Weichselian), similar to straighttusked elephants^{17,18}. For comparison, 15 fossils of woolly mammoth (*Mammuthus primigenius*) and woolly rhino (Coelodonta antiquitatis) from the same or geographically close localities in the Upper Rhine Graben were subjected to ¹⁴C analysis, too. Their estimated dates similarly range between 47 and 31 cal ka and there is no temporal separation between them and hippos (Figure 2, Table S2). To test this further, enamel-based amino acid geochronology was undertaken on three hippo specimens from Eich. The results are not inconsistent with a post-Eemian age for the hippos; however, assigning a definitive MIS3 age is not possible due to the lower temporal resolution of this method for this period (see STAR Methods, Figure S3). Besides hippos, Upper Rhine Graben gravel pits also yielded several other species usually associated with temperate (i.e., interglacial) conditions but without any taphonomic differences to fossils from cold-adapted species that could indicate large-scale temporal differences (e.g., Eemian vs. MIS3; see STAR methods, Figure S3). This interpretation fits with the absence of sediment layers of Eemian age in the Upper Rhine Graben (see STAR Methods). Together, the dating analyses suggest that, during MIS3, hippos either were broadly contemporaneous with large mammals generally accepted as cold-adapted or, more likely, that hippos and woolly mammoths/rhinos may have cyclically alternated in the Upper Rhine Graben on a short temporal scale not resolvable by our data. This would imply repeated short-term colonization of the Upper Rhine Graben by hippos, for instance during interstadials (although our radiocarbon dating results do not allow assignment of the hippo fossils to precise interstadials). In either case, Late Pleistocene fossil localities in the Upper Rhine Graben seem not to preserve the Eemian interglacial – Weichselian glacial transition.

While hippo presence in central Europe during MIS3 might be surprising, it is not implausible or unlikely. The middle Weichselian is known for its interstadial complex, which includes multiple short interstadial phases resulting in the stagnation of inland ice shield growth 19-21. The published pollen record from the Upper Rhine Graben and surrounding lower mountain regions shows evidence of plants indicative of temperate, partly forested conditions during MIS3 interstadials^{22–29}. To provide further support for this, we obtained radiocarbon dates of fossil wood pieces from gravel pits geographically close to those the hippo samples originated from. The dates confirm the presence of cold- (pine) and temperate-associated (oak) tree species in the Upper Rhine Graben during MIS3 (Table S2). Previous analyses from sediments and invertebrate remains similarly suggest multiple warm phases during this period^{30–33} Altogether, the Upper Rhine Graben offered a localized microclimate during several phases of MIS3 that was favorable for sheltering species that require more temperate conditions with relatively mild temperatures. These conditions would have been sufficient to prevent the complete freezing of water bodies and to provide enough vegetation cover for foraging hippos (and likely other temperate-associated species) also during winter. The Upper Rhine Graben might represent the easternmost region with such climate conditions that were suitable for hippo survival and potentially the only one in central Europe during MIS3, as hippos did not spread farther to the east during the Late Pleistocene^{3,4,8}. At the end of MIS3, interstadials were much less common and the lack of interstadials at the transition to the last glacial maximum¹⁹⁻²¹ likely led to the final extinction of hippos from central Europe.

A small population colonized the Upper Rhine Graben

157

158

159

160

161

162163

164

165

166167

168

169170

171

172

173

174

175

176

177178

179

180

181

182

183

184 185

186

187

188

189

190

191

192

193

194 195

196 197

198

199

200201

202

203

Radiocarbon ages of the fossil hippos allowed us to further trace the origin of these late-surviving hippos from the Upper Rhine Graben. We performed Bayesian temporal calibration with the mitogenome dataset, associated tip dates and two tree prior models that both have been shown to best accommodate for mixed inter- and intraspecific sampling³⁴. Using a Bayesian skyline coalescence tree prior, the basal node within African-European H. amphibius was dated to 834 ka (95% highest posterior density [HPD] 380 ka-1.6 million years ago; Figure 1C). The earliest coalescence among hippos from the Upper Rhine Graben was estimated to 228 ka (95% HPD 96-400 ka). Applying a Birth-Death tree prior resulted in similar median values for the respective node ages (948 ka and 242 ka, respectively) but broader HPDs (Figure S2). These divergence dates were also similar when only the three Upper Rhine Graben samples with higher mitogenome completeness (>60%) were included (Figure S2). The basal coalescence within H. amphibius broadly coincides with a period of initial intraspecific diversification and geographic expansion in the African common hippo as previously shown by molecular and paleontological evidence^{35–39}. The coalescence among Late Pleistocene hippos from the Upper Rhine Graben provides a genetic proxy for the colonization and expansion in Europe. The temporal range of this node fits with the oldest putative fossils of *H. amphibius* in Europe from Middle Pleistocene deposits in Italy dating to ~450 ka or younger^{10,40,41}. Hippos spread across western and central Europe during subsequent interglacial periods, probably using larger Rhône and Rhine rivers as major routes of dispersal^{1,2}. Their presence in central and western Europe during the Holsteinian and Aveley interglacials, however, is disputed and a definitive fossil record of H. amphibius did not emerge before the Eemian^{1,42}. Whether hippos were also present in the Upper Rhine Graben and central Europe in general during the cold periods of the early Weichselian (MIS4) remains unknown but seems unlikely given the near lack of interstadials between 60 and 70 ka²¹. Nevertheless, hippo fossils dating to MIS4 (and potentially younger) are known from the Iberian⁴³ and Italian peninsulas¹⁰,

which might have been the source for the Upper Rhine Graben population in central Europe during the middle Weichselian (MIS3). Eemian and middle Weichselian presence of hippos in western and central Europe thus likely represent different expansion events from southern European refugial areas.

This colonization of the Upper Rhine Graben in central Europe during MIS3 then likely imported the deep mitogenetic lineages (>200ka) from longer persisting source populations in southern Europe. Such patterns of genetically divergent lineages in close spatial and temporal proximity resemble those seen in other Late Pleistocene mammals in central and western Europe, such as giant deer, woolly rhinoceros and mammoth^{44–46}, and might be the result of periodical colonization of central Europe⁴⁷. We further evaluated the genetic status of this late colonizing population by inferring genome-wide diversity in the NK37 paleogenome. Based on post-mortem damage patterns and X chromosomebased recalibration, heterozygosity (θ) was estimated in 1Mb windows across all autosomes for the nuclear dataset above (Figure S1). Despite the low coverage (0.47x) of the Upper Rhine Graben sample NK37, heterozygosity estimates were robust even when down-sampled to 0.1x coverage (Figure 3). Estimates in the sample NK37 ($\theta_{mean} = 0.00121$) and the West African pygmy hippo WPH1 ($\theta_{mean} =$ 0.000843) are considerably lower than in the two African common hippos (ACH1 θ_{mean} = 0.00486; ACH2 θ_{mean} = 0.00431). Extant West African pygmy hippos are today restricted to the Upper Guinea Forest of western Africa and are fragmented into isolated populations⁴⁸. The similarly low genome-wide heterozygosity estimated from the sample NK37 thus suggests that hippos from the Upper Rhine Graben also represented a small, isolated population^{49–51}.

Conclusion

Middle and Late Pleistocene climate fluctuations resulted in fundamental changes of the environment and its inhabiting large mammal fauna^{5,12,52}. Glacial and interglacial faunas alternately colonized this area during favorable climate conditions from their core areas in north-eastern and southern Europe, respectively, when climate conditions were favorable for them. Nevertheless, neither the timing of colonization and extinction in central Europe nor the phylogenetic relationships to their African relatives could be resolved until now for Late Pleistocene hippos, although they were assumed to be the prime indicator of interglacial conditions.

Here we approached this issue by combining paleogenomics with radiocarbon dating of putative Eemian hippos from the Upper Rhine Graben. These turned out to be part of the previously much more widely distributed extant African common hippo, although genome-wide data for more Pleistocene European as well as extant African common hippos will be needed to disentangle their complex relationships. Contrary to the traditionally accepted view, our newly dated bone remains reveal that hippos did not disappear in central Europe at the end of the Eemian as previously thought. A small population instead recolonized the central European Upper Rhine Graben during MIS3, likely from southern Europe. We thus could show that interstadial phases provided a temperate refugium allowing an (at least temporary) immigration of hippos (and likely other interglacial elements) in the middle of the last glacial period. Overall, the late presence of hippos in the Upper Rhine Graben suggests that fossils from other putative Eemian sites should be re-analyzed as well to evaluate if this species also survived into the last glacial elsewhere in western and central Europe (e.g., the Netherlands⁵³).

Resource availability

248

247

- 249 Lead contact
- 250 Further information and requests for resources and reagents should be directed to and will be fulfilled
- by the lead contact, Patrick Arnold (patrickarnold@uni-potsdam.de).

252

253

- Materials availability
- 254 This study did not generate new unique reagents.

255

257

258

259

260

261

262

263

264

265

- 256 Data and code availability
 - All raw sequencing data produced in this study data have been deposited at NCBI GenBank as BioProject PRJNA1105865 and are publicly available as of the date of publication. All amino acid data from this study have been deposited at the NOAA repository and are publicly available as of the date of publication (https://www.ncei.noaa.gov/pub/data/paleo/aar/). For the purpose of open access, a Creative Commons Attribution (CC BY) license is applied to any Author Accepted Manuscript version arising from this submission.
 - This paper does not report original code.
 - Any additional information required to reanalyze the data reported in this paper is available from the lead contact upon request.

266

267

268

Acknowledgments

- This project was conducted within the framework of the research project "Eiszeitfenster Oberrheingraben" ("Ice Age Window Upper Rhine Graben" (2016-2022)), funded by the Klaus Tschira
- 271 Stiftung gGmbH Heidelberg. L.D. acknowledges support from the Swedish Research Council (2021-
- 272 00625) and the European Union (ERC, PrimiGenomes, 101054984). D.W. acknowledges support from
- the Swiss National Science Foundation (310030_200420). The authors also acknowledge support from
- 274 Science for Life Laboratory, the Knut and Alice Wallenberg Foundation, the National Genomics
- 275 Infrastructure funded by the Swedish Research Council, and Uppsala Multidisciplinary Center for
- 276 Advanced Computational Science for assistance with massively parallel sequencing and access to the
- 277 UPPMAX computational infrastructure.

278

279

280

Author contributions

- Conceptualization, P.A., W.R., and M.H.; methodology, P.A., F.A., D.D., J.L.A.P., A.F., D.W., A.B., W.R.,
- and M.H.; investigation, P.A., F.A., D.D., S.L., C.H., R.F., I.H., M.D., and A.F.; formal analysis, P.A., F.A.,
- 283 D.D., S.L., C.H., R.F., M.D., K.P., and A.F.; writing original draft, P.A., D.D., R.F., S.L., C.H., I.H.; writing

284 285	- review & editing, P.A., D.D., J.L.A.P., L.D., A.F., D.W., A.B., R.F., W.R., M.D., K.P., and M.H.; resources, D.D., L.D., and W.R.; visualization, P.A., D.D., R.F., and A.F.; supervision, A.B., W.R., K.P., and M.H.
286	
287	
288	Declaration of interests
289	The authors declare no competing interests.
290	
291	

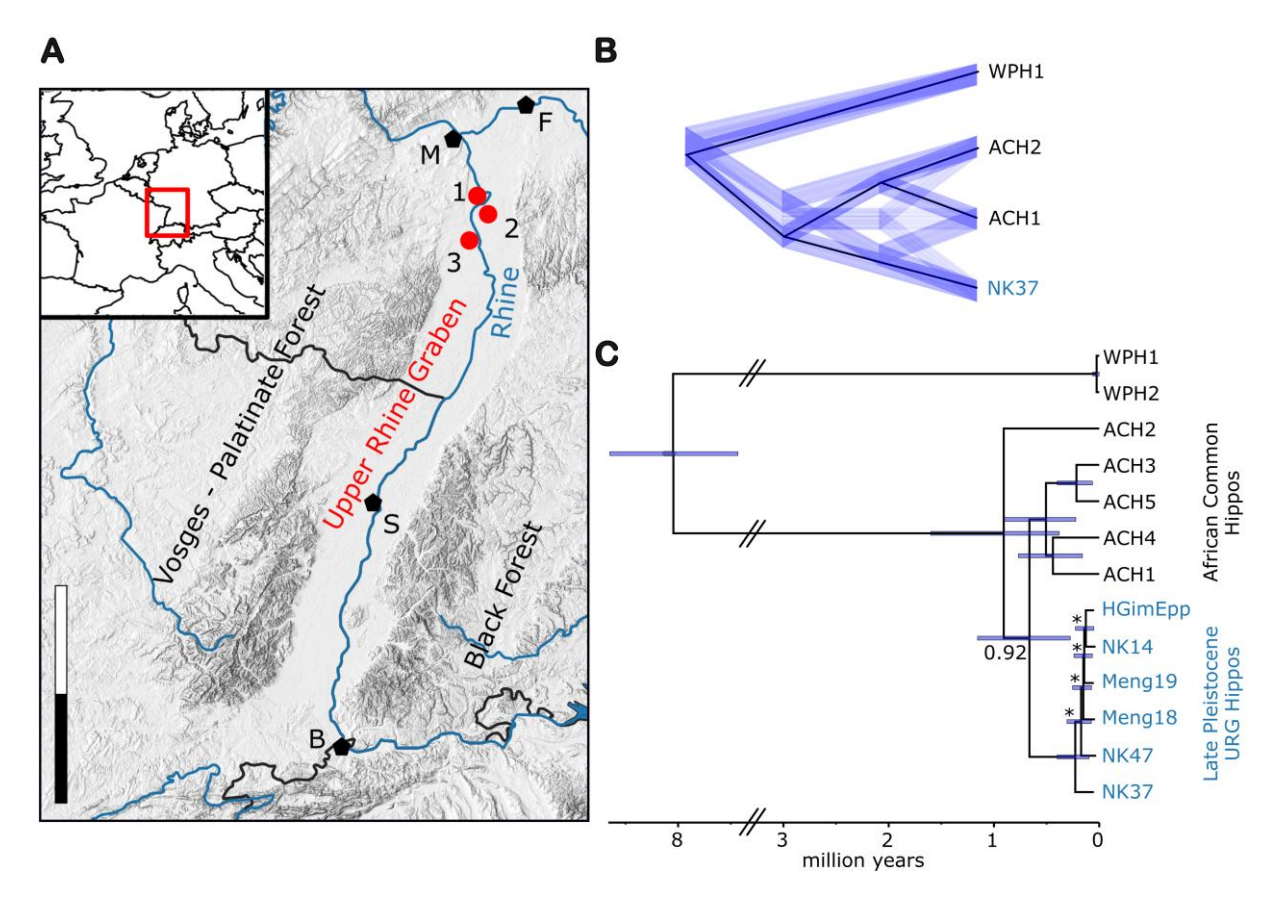


Figure 1 Geographic origin and phylogenetic relationships of fossil hippos from the Upper Rhine Graben.

A) Location of gravel pits in the Upper Rhine Graben in southwestern Germany where the analyzed fossils of hippos, mammoths and woolly rhinos have been unearthed (red dots): 1 Gimbsheim/Eich, 2 Groß-Rohrheim, 3 Bobenheim-Roxheim. Black pentagons indicate major cities: B Basel, F Frankfurt, M Mainz, S Strasbourg. Scale: 100km in total. B) Nuclear phylogeny based on 3,085 genomic windows (with uniform branch lengths) including a single ancient sample (NK37) from the Upper Rhine Graben. Maximum Likelihood tree from concatenated data set in black (100% bootstrap support), densitree visualization of incongruence among window trees in blue (with uniform branch lengths). C) Calibrated Bayesian phylogeny of mitochondrial genomes from Late Pleistocene Upper Rhine Graben (URG) hippos, extant African common hippos (ACH) and extant West African pygmy hippos (WPH) using a Bayesian skyline coalescent tree prior. Node support (Posterior Probability) is >0.99 for all nodes except those indicated differently or marked with an asterisk (<0.75).

See also Figure S1-S2 and Table S1.

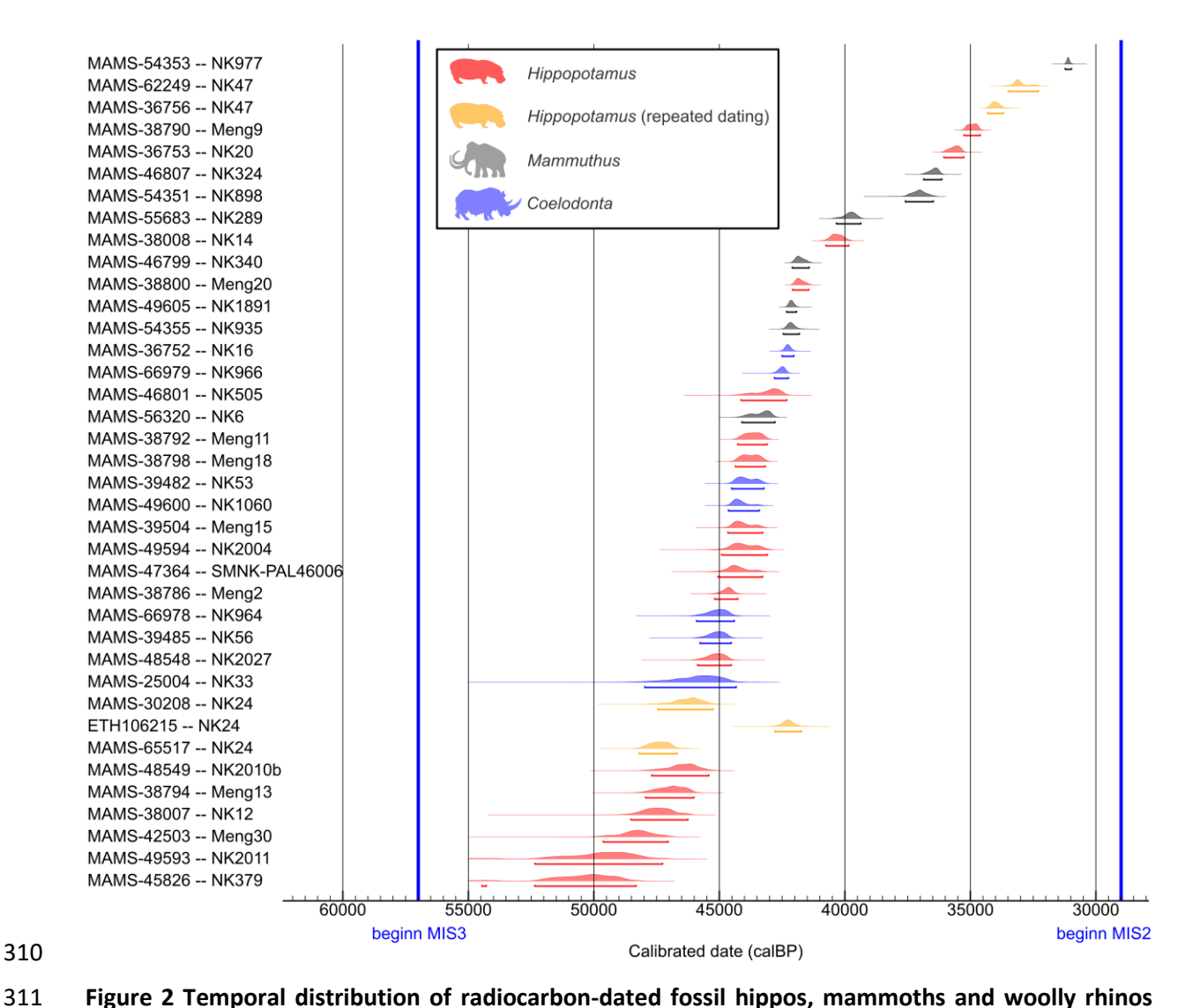


Figure 2 Temporal distribution of radiocarbon-dated fossil hippos, mammoths and woolly rhinos from the Upper Rhine Graben.

Probability distributions of radiocarbon dates for fossil hippos (*Hippopotamus*, red), woolly mammoths (*Mammuthus*, gray) and woolly rhinos (*Coelodonta*, blue). Repeated estimates for two hippo specimens (NK47 and NK24) in orange. Estimates for eight additional hippos were beyond the limit of radiocarbon dating (>49 ka). Blue lines mark the boundaries of marine oxygen isotope stages (MIS).

See also Figure S3 and Table S2.

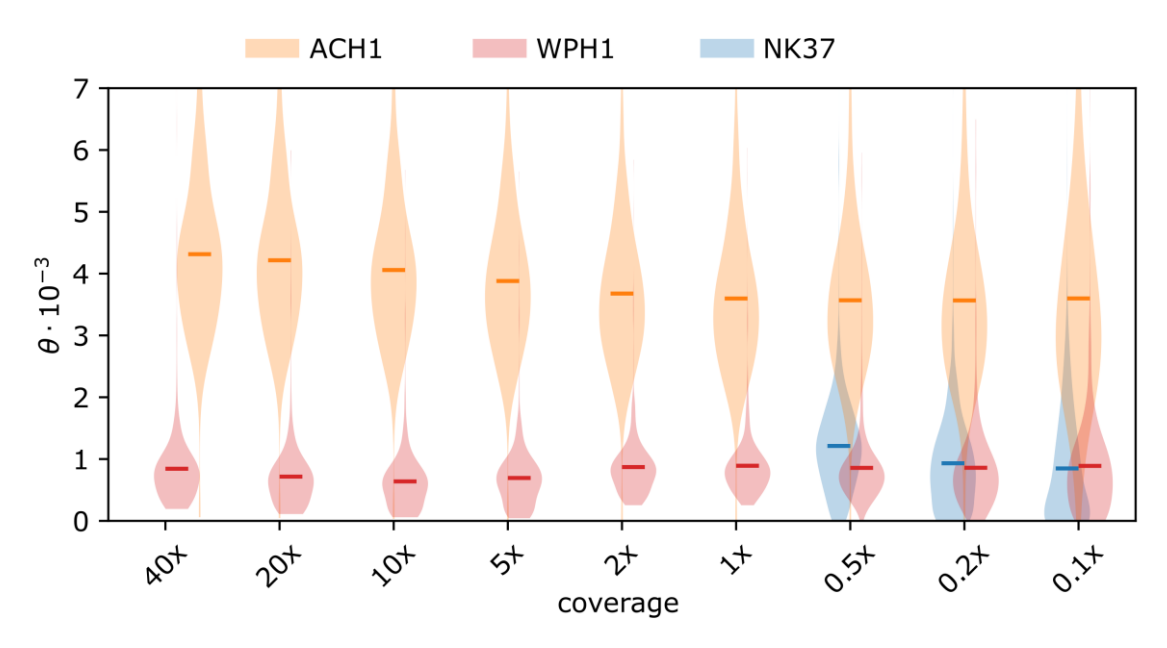


Figure 3 Genome-wide heterozygosity (θ) across different genomic coverage.

Estimates for one African common hippo (ACH1), one West African pygmy hippo (WPH1) and Upper Rhine Graben sample NK37. Step-wise down-sampling of genomic coverage from original data (left) to as low as 0.1X. Results suggest estimates to be robust even down to 0.1x coverage.

See also Figure S1 and Table S1.

STAR Methods

Experimental model and subject details

Origin of samples and taphonomy

The faunal remains originate from gravel pits in Eich, Gimbsheim and Bobenheim-Roxheim (all Rheinland-Pfalz), and near Groß-Rohrheim (Hessen) in the Upper Rhine Graben of southwestern Germany (Figure 1). Today, the majority of remains are housed in the "Reis Collection" (Klaus Reis, Deidesheim), which comprises about 15,000 remains collected prior to 1984. Since 2016, the collection has been archived in the Reiss-Engelhorn Museen in Mannheim⁵⁴. Additional faunal remains of this study originate from other museums and collections (Tables S1-S2). Besides hippos, the faunal assemblages of these sites in the Upper Rhine Graben include several 'interglacial' and 'intermediate' elements (*sensu* von Koenigswald¹²), including *Panthera spelaea* (cave lion), *Palaeoloxodon* (*Elephas*) antiquus (straight-tusked elephant), *Equus sp.* (wild horse), *Sus scrofa* (wild boar), *Bos primigenius* (aurochs), *Bubalus murrensis* (water buffalo), *Cervus elaphus* (red deer), *Capreolus capreolus* (roe deer), *Megaloceros giganteus* (giant deer), *Dama dama* (fallow deer), *Alces alces* (elk), *Stephanorhinus hemitoechus* (steppe rhinoceros), and *Stephanorhinus kirchbergensis* (forest rhinoceros). No systematic bias regarding breakage, completeness and rolling is observable between hippo and other 'interglacial' species versus woolly mammoth/woolly rhino and other glacial species (Figure S3).

Geological setting and stratigraphy

The Upper Rhine Graben (Figure 1) is one of the most important rift systems in Europe and offers an outstanding sediment trap where a continuous accumulation and preservation of fossils is documented from the Eocene to the Holocene¹¹. The long history of quarrying activities in the sandygravelly Upper Rhine Graben deposits (Mannheim formation) unearthed numerous fossils of large mammal remains from the Late Pleistocene. Over the last two decades, our understanding of the Mannheim formation has been revised. The Upper Rhine Graben is a south-southwest to northnortheast striking rift structure that is part of the European Cenozoic Rift System extending from the Mediterranean Sea to the Lower Rhine Embayment⁵⁵. The Upper Rhine Graben can be divided into two parts: a southern part from Basel to Karlsruhe and a northern part from Karlsruhe to Mainz. The differences between the two parts are lateral internal rift-structures with different subsidence. Since the River Rhine acted as the only drainage system that connected the Alps with the North Sea, the Upper Rhine Graben acts as a major sediment trap. Therefore, the Upper Rhine Graben offers unique potential for a continuous sediment accumulation and preservation. Continuous subsidence permitted the accumulation of about 300 m of Quaternary sediments in the area west of Heidelberg, the socalled "Heidelberg basin"⁵⁶. In the northern Upper Rhine Graben, the upper Quaternary sediments, sand and gravel deposits alternate with clay layers in between. Aiming to provide a better understanding of the geological evolution of the northern Upper Rhine Graben (especially the Heidelberg basin), and its control by climate change and tectonics, and for the correlation of alpine and north European glacial evolution, the Heidelberg Basin Drilling Project was initiated in 2002⁵⁷. The investigations are primarily based on three newly cored boreholes drilled from 2002 until 2008.

By working on various research boreholes in the northern Upper Rhine Graben, a new lithostratigraphic concept could be developed for the Pliocene and Pleistocene sediments of the northern Upper Rhine Graben⁵⁸. Four formations could be defined^{11,57}. The Mannheim Formation completes this lithological sequence. It has a Middle to Late Pleistocene age and mostly starts with a

coarse sediment pulse. Several fluvial aggradation cycles follow. Fine-grained floodplain or overbank deposits are often not preserved. Mass deposits of gravel, cobbles, blocks, and diamictons occur at the graben boundaries and at the entry of the Neckar River into the Upper Rhine Graben. The thickness of the Mannheim Formation varies between a few meters and up to 60 m in the subsidence center of the Heidelberg Basin. The heavy mineral fraction of the fine sands within the Mannheim Formation is characterized by an alpine spectrum with unstable heavy minerals such as garnet, epidote, green hornblende, and alterite. This spectrum also dominates local inputs with stable heavy minerals such as zircon, tourmaline, and rutile. A luminescence age on sediments from a core in Kronau about 20 km south of Heidelberg, outside the Heidelberg Basin, at the transition from the Ludwigshafen to the Mannheim Formation, shows an age of 470 ± 41ka, which is correlated with MIS 12⁵⁹. In this location, ages correlated with MIS 10, 8, 6, 4, and 2 were also dated. Thus, up to six accumulation phases could be shown for Kronau. However, this interpretation is based on only a few dates and must be validated with further luminescence dating. Nevertheless, these datings correspond well with magnetostratigraphic studies⁶⁰, according to which the Ludwigshafen and Mannheim Formations can be assigned to the normally polarized Brunhes Chron. In recent decades, a large number of research boreholes have been drilled in the northern Upper Rhine Graben^{11,56}, several of them allowing better interpretation of the younger sediments and their respective layers. Various boreholes have also been palynologically analyzed. So far, no sediments from the Eemian period were identified 11,61,62. Data from optically stimulated luminescence (OLS) dating confirm the lack of Eemian sediments in the Mannheim Formation of the Upper Rhine Graben^{63,64}. The upper 33m of sediment cores (fitting with the maximum dredging limit in gravel pits) were deposited during the last glacial period (Weichselian, <60 ka), according to OSL dating⁶³.

392

393

394

395

396

397

398 399

400

401

402

403

404

405

406

407

408

409

410

411

412

413

414

415

391

370

371

372

373

374

375

376

377

378

379

380

381

382

383 384

385

386

387 388

389 390

Method details

Radiocarbon dating

Radiocarbon dating was performed at the radiocarbon laboratory of the Curt-Engelhorn-Center Archaeometry (CEZA) in Manheim⁶⁵ by extracting collagen according to a modified Longin extraction⁶⁶ from hippopotamus bone and tooth samples as described in detail in Lindauer et al.⁶⁷. The pretreatment typically starts by applying organic solvents to remove varnish that was applied to most of the bone material for conservation purposes by the collectors, followed by an acid step to remove carbonates, a base step to remove soluble humic acids, and a final acid step to remove any newly accumulated atmospheric contaminating carbon dioxide. The sample was then gelatinized in hydrochloric acid at pH 3 at 60 °C for 20 hours. The remaining solid material was then removed using an Ezee - Filter (Elkay) before ultrafiltration (Vivaspin Turbo 15) of the collagen to remove shortchained contamination. The sample was then freeze-dried, combusted in an elemental analyzer (MicroCube, Elementar) and graphitized to elemental carbon using in-house or commercially available graphitization systems (AGE3, IonPlus). The graphite was then pressed into a target and measured in a MICADAS-type accelerator mass spectrometer system (AMS). The results were fractionationcorrected (to δ^{13} C=-25 per mil) using the δ^{13} C values measured at the AMS. The conventional radiocarbon dates were calibrated using the calibration curve IntCal2020⁶⁸ and the software OxCal 4.4^{69} .

The impact of conservation chemicals of unknown composition with which the fossil specimens have been treated in historical time has been systematically evaluated previously by the authors¹⁶. Additional samples from the Reis collection for which suitable amounts of varnish could be collected were tested here. We removed the upper bone layers and dated the varnish of samples NK37 (hippo;

MAMS-47983) and NK25 (cave lion; MAMS-47982) to conventional ¹⁴C ages of 30,011 ± 150 and 36,928 ± 262 years BP, respectively. Those results are comparable to the previously published date for the varnish of NK34 (muskox; MAMS-39641) with a conventional ¹⁴C age of 30,958 +- 203 years BP¹⁶. For varnish contamination to significantly affect the ¹⁴C age of the bone material, the varnish chemicals would need to survive the sample pre-treatment, particularly the ultrafiltration step, in large quantities while still producing collagen of good condition. However, since all datable samples yielded visibly identifiable collagen with good collagen yields of above 1% up to 10%, we conclude that only negligible amounts of varnish (if any) might have remained in the extract. In the three samples tested, ¹⁴C dates were always different between varnish and cleaned bone. This indicates significant removal of varnish contamination, especially considering the fact that a number of samples produced infinite ¹⁴C ages.

To ensure the accuracy of dating, the two hippo samples with most material left underwent repeated ¹⁴C testing (Figure 2) at CEZA and the radiocarbon laboratory of ETH Zurich, Switzerland, using the same protocol as above. For NK47, both results (measured at CEZA) show reasonable consistency despite not being identical within their margins of error, yielding conventional ¹⁴C ages of 29,398 +- 117 and 28,690 +- 90 years BP, respectively. NK24 was dated twice at CEZA and once at ETH Zurich, with greater variability compared to NK47. While the CEZA results for NK24 are relatively close to each other (43,833 + 484 years BP and 45,060 + 230 years BP, respectively), the ETH Zurich result is even notably younger (37,975 + 550 years BP). Nevertheless, all dating repetitions confirm the MIS3 age of the hippo fossils. Additional FTIR spectral analysis was conducted on a Spotlight 200i system (PerkinElmer, Waltham MA, USA) at the ETH laboratory for the sample prepared there following Haijdas et al.⁷⁰ (Figure S3).

Fossil wood pieces were not covered by lacquer or varnish. They underwent a standard ABA (acid-base-acid) pretreatment with 2M hydrochloric acid (HCl) and 4% sodiumhydroxid (NaOH) followed by 2M HCl again to remove limestone and soluble humic acids⁷⁰. Subsequent steps for graphitization and measurement were the same as described for bone above.

Amino acid geochronology

Three hippo tooth enamel samples from Eich, Upper Rhine Graben, and seven from Barrington, Britain for comparison (Figure S3, Table S2) were prepared using established protocols for intra-crystalline protein analysis of enamel⁷¹. Enamel chips were mechanically cleaned to remove adhesive residues and non-enamel dental tissues, then powdered and subjected to a 72-hour bleach treatment to isolate the closed-system protein fraction. Each sample was divided into two subsamples: one was analyzed for free amino acids (FAA), while the other was hydrolyzed to determine total hydrolysable amino acids (THAA). Samples were demineralized in HCl before the pH was raised with KOH and the solution centrifuged, producing a biphasic separation; the supernatant was extracted, dried via centrifugal evaporation, and rehydrated in an internal standard. Samples were analyzed in preparative duplicate by reverse-phase high-performance liquid chromatography, with standards and blanks run alongside. Due to deamination during hydrolysis, aspartic acid and asparagine were recorded together as Asx, and glutamic acid and glutamine as Glx. Racemization ratios of Asx, Glx, phenylalanine, and alanine were used to construct intra-crystalline protein decomposition (IcPD) profiles, exploiting their differential racemization rates for temporal resolution. Comparison of FAA and THAA D/L values were used to assess the extent of closed-system behavior, with significant divergence suggesting possible contamination or diagenetic alteration. To date, no hippopotamus enamel from Germany has been analyzed for its intra-crystalline protein decomposition (IcPD). Consequently, the hippo enamel from Eich has been compared with an established enamel chronology for elephantids (Palaeoloxodon and Mammuthus) from Britain⁷², as well as a smaller set of British hippo enamel specimens attributed to the Eemian based on the pollen assemblage, optical spin luminescence dates and opercula-based amino acid racemization dating^{73–76}. The attribution of *H. amphibius* remains to MIS5e sites in Britain is therefore likely more robust than on the European mainland, owing to Britain's isolation^{77,78}.

Differences in the underlying protein sequences between taxa lead to consistently different rates of racemization, limiting direct comparison across species⁷². The IcPD values of the Eich hippo enamel were therefore also compared to hippo enamel from a British site (Barrington beds) correlated with the Eemian. As racemization rates are temperature-dependent, regions that experienced a significantly different integrated temperature history will exhibit different rates of IcPD. However, recent opercula-based dating shows that there is only a slight difference in IcPD between last interglacial sites in Britain and near the Upper Rhine Graben⁷⁹ (as no interglacial sediments are directly available from the Upper Rhine Graben), suggesting that the even-slower racemizing enamel from Britain is likely to be comparable to parts of south-western Germany in terms of racemization behavior. As racemization values from the Eich hippo specimens are similar to those of British hippos (Figure S3), a comparison is between both geographic regions is valid (within the limitation of taxon-specific differences). When compared to the larger British elephantid time series dataset, the IcPF values of the Eich hippo enamel fall between those samples from MIS4/3 and MIS53 (Eemian), although closer to the former (Figure S3). However, because of the slow rates of racemization in enamel, the confidence intervals of IcPD for MIS4/3 elephantids are relatively large and partially overlap with those of MIS5e elephantids; this is likely to also apply to hippos. Therefore, a post-Eemian age for the Eich hippo samples is possible but cannot currently be confirmed by amino acid racemization dating alone due to the lower temporal resolution of this enamel-based method for this period.

484 Ancient DNA laboratory methods

All pre-amplification steps were carried out in the dedicated ancient DNA facilities at the University of Potsdam, including negative controls for both extraction and library preparation. In a first round of screening, ~50 mg of bone powder per sample were collected using a Dremel Fortiflex (9100-21) and a 2.4- to 2.8-mm-diameter drill bit. DNA was extracted following a protocol optimized for highly fragmented DNA⁸⁰. A total amount of 13 ng of DNA for each extract was initially treated with USER enzyme for 15 minutes at 37° C (modified from Meyer et al.⁸¹) to remove uracil residues resulting from cytosine deamination. The USER-treated extracts were then converted into single stranded libraries using the protocol described in Gansauge et al.82. The resulting libraries were then amplified and dualindexed. PCR cycles for amplification were determined in advance using qPCR analysis of the unamplified library. Concentration and length distribution were determined using Qubit 2.0 and 2200 TapeStation (Agilent Technologies), respectively. The single-stranded libraries were sequenced on an Illumina NextSeq500 system⁸³ at the University of Potsdam in 75bp single-end mode for five to 20 million reads. A single sample (NK37) yielded sufficient endogenous DNA to sequence its (nonenriched) library for 3 billion reads on an Illumina NovaSeq6000 system at the SciLifeLab, Stockholm, in 100bp paired-end mode. Libraries were additionally enriched for mitochondrial DNA by two rounds of in-solution hybridization capture using the Arbor Biosciences MyBaits kit according to the manufacturer's instructions (Manual v4.01, April 2018). Enrichment capture baits were designed based on the mitochondrial reference genome of the African common hippo (Genbank: NC 000889.1). Enriched libraries were amplified following the amplification steps used in Taron et al. 84 and then sequenced again on an Illumina NextSeq500 system at the University of Potsdam in 75bp single-end mode.

462

463

464

465

466

467 468

469

470

471

472

473

474

475

476

477

478

479

480

481

482

483

485

486

487

488

489

490 491

492 493

494

495

496

497 498

499

500

501

502

503 504

Quantification and statistical analysis

Nuclear genome phylogeny and gene flow

The nuclear data set consisted of sequencing data for one ancient sample (NK37) and three previously published modern hippos (ACH1, ACH2, WPH1; Table S1). Adapter sequences and low-quality bases (< Q30) were trimmed and reads shorter than 30bp removed with cutadapt 1.1885. Untrimmed reads were discarded. Paired reads were merged with flash 1.2.1186. For NK37, only merged reads were subsequently mapped to the West African pygmy hippo reference genome (GenBank: GCA_023065765.1) using BWA 0.7.1787 -aln with relaxed mapping parameter (-n 0.01). Reads with a mapping quality below 30 were removed using Samtools 1.15.188. Duplicate reads were identified program MarkDuplicatesByStartEnd.jar (https://github.com/dariober/Javajava cafe/tree/master/MarkDupsByStartEnd) and removed. For ACH1, ACH2 and WPH1, merged and unmerged reads were mapped to the West African pygmy hippo reference genome (GenBank: GCA_023065765.1) using BWA 0.7.17 -mem⁸⁹. Duplicate reads were identified using picard 2.18.29 (http://broadinstitute.github.io/picard/). For the sliding window tree analyses, we generated pseudohaploid sequences using random read sampling (-doFasta 1) in ANGSD 0.935⁹⁰ and the following parameter settings: -minQ 30, -minMapQ 30, -uniqueonly 1, -only_proper_pairs 0, -remove_bads 1, baq 2, -C 0, -explode 1, -doCounts 1, -trim 0. We ran a sliding window tree analysis91 using WindowTrees v1.0.0 (https://github.com/achimklittich/WindowTrees) in binary mode to exclude transitions (—binary), with a missing data threshold of 50% (-N 0.5), a window size of 5kb (-w 5000) and a gap size of 5kb between windows (-lw 5000). Topological incongruence among window trees were visualized as densitree with the phangorn 2.5.5 package⁹² in R. A Maximum Likelihood tree was computed from concatenated windows in IQTREE 2.0.3⁹³ using the Jukes-Cantor model for binary data. To test for gene flow, D-statistics were calculated using ANGSD 0.935 (-doAbbababa), with the WPH1 as outgroup and NK37, ACH1 and ACH2 as P1, P2 and P3, respectively, and the following settings: doCounts 1, -useLast 1, -rmTrans (use only transversion sites), -minQ 30, -minMapQ 30, -uniqueonly 1, -remove_bads 1, -baq 2, -setMinDepth 3. Standard errors estimation using jackknife procedure was done on block size of 5 Mb. Z-scores > 3 were defined as significant.

535536

537

538

539

540541

542

543

544

545

546547

548

549

550

551552

508

509

510

511512

513514

515

516

517

518

519

520

521

522523

524

525526

527

528

529530

531

532

533

534

Mitochondrial phylogeny and networks

Adapter sequences and low-quality bases (< Q30) were trimmed with cutadapt 1.18. Untrimmed reads were discarded. An individual minimum length cut-off was determined empirically for each library as described previously⁹⁴ (Table S1). Trimmed reads were subsequently mapped to the nuclear (GenBank: GCA_023065835.1) and mitochondrial genome (GenBank: NC_000889.1) of the African hippopotamus using BWA aln 0.7.17 with relaxed mapping parameter (-n 0.01). Reads with a mapping quality below 30 were removed using Samtools 1.15.1. Duplicate reads (reads with the same start and end identified using the java program MarkDuplicatesByStartEnd.jar (https://github.com/dariober/Java-cafe/tree/master/MarkDupsByStartEnd) and removed. Cytosine deamination patterns and length distribution of resulting reads were calculated using mapDamage 2.1.095. (Figure S1). Mitochondrial consensus sequences were called using Samtools 1.15.1 with 85% majority rule for base calling and minimum coverage of 2x. Consensus calling was also repeated with minimum coverage of 3x. Consensus sequences were manually checked for premature stop-codons in aliview 1.26%. Mitogenomes of living hippos have either previously been published or were here assembled de-novo from available sequencing data (Table S1). For the latter, paired-end sequencing reads were trimmed with cutadapt 1.18 and assembled with NOVOPlasty 4.3.197 with default parameters.

Ancient and modern mitochondrial genomes were aligned using MAFFT v7.31098. Poorly-aligning parts of the D-loop were removed from the alignment resulting in a total alignment length of 16,126 bp. The optimal set of partitions and substitution models under the Bayesian information criterion from all possible combinations of rRNAs, tRNAs and the individual codon positions of protein coding genes was determined using ModelFinder⁹⁹ as implemented in IQTREE 2.0.3. A Maximum Likelihood phylogenetic tree with 1000 ultrafast bootstrap¹⁰⁰ replications was reconstructed in IQTREE 2.0.3 from the resulting three partition scheme. Results of the phylogenetic reconstruction were consistent using different minimum coverage limits for consensus calling (Figure S2). All subsequent analyses were therefore done with consensus mitogenome sequences with minimum coverage of 2x. The Maximum Likelihood reconstruction was rerun but with constraining Upper Rhine Graben hippos to fall outside all extant African common hippos. The likelihood of both trees (Upper Rhine Graben hippos outside or inside African common hippos) were then compared using the approximately unbiased test¹⁰¹ as implemented in IQTREE 2.0.3. We additionally used two larger datasets from partial mitochondrial sequences in order to capture the genetic diversity of the extant African common hippo¹⁵. The first dataset contains 854 bp of cytochrome b from 23 individuals (GenBank: KR005049-KR005071). The second dataset contains 929 bp of tRNA-Pro, the control region and tRNA-Phe from 66 individuals (GenBank: KR004948-KR005044). Respective sequences from Upper Rhine Graben hippos (if preserved) were added to the datasets and minimum-spanning haplotype networks were reconstructed in PopArt 1.7¹⁰² (Figure S2).

572

573

574

575

576

577

578

579

580

581

582

583 584

585

586 587

588

589 590

553

554555

556

557558

559

560

561

562

563

564

565

566567

568

569

570

571

Time-calibrated Bayesian analysis

To estimate the divergence time among late Pleistocene hippos from the Upper Rhine Graben as well as to extant African common hippos, a time-calibrated Bayesian analysis was performed in BEAST 2.7.2¹⁰³ using the same alignment and partition scheme as for the Maximum Likelihood phylogenetic reconstruction above. Pleistocene samples in the alignment were fixed at their above calibrated radiocarbon dates. Samples dated to beyond the radiocarbon limits (>49 ka) were fixed to 59 ka as their presence in the Upper Rhine Graben during MIS4 is unlikely given the near lack of interstadials before 60 ka²¹. The divergence between H. amphibius and C. liberiensis was set to 8.1 Ma (normal distribution prior with a mean of 8.1 Ma and a standard deviation of 310 ka) as node calibration following previous estimates 104,105. The analysis was run using a Bayesian skyline coalescent tree prior and lognormal relaxed clock models for each partition. As population structuring among and within species may violate the assumptions of the Bayesian skyline coalescent model, the divergence dating analysis was replicated using a Birth-Death speciation tree prior. Both tree prior models, however, have been shown to best accommodate for mixed inter- and intraspecific sampling³⁴. The MCMC chain was run for 50 million generations. Convergence and adequate sampling (ESS > 200) of all parameters were verified in Tracer 1.5.0.52¹⁰⁶. The first 10% of trees were removed as burn-in, and the maximum clade credibility trees obtained from the posterior sample, with node heights scaled to the median of the posterior sample, using TreeAnnotator 2.7.1.

591

592

593 594

595

596

597

598

Genomic-wide heterozygosity analysis

Nuclear data sets including NK37, ACH1, ACH2 and WPH1 were processed with the Gaia part of the ATLAS¹⁰⁷ pipeline (bitbucket.org/wegmannlab/atlas-pipeline, commit f3db9e3). For sample NK37, the analysis was restricted to the first mates since most reads did not have a second mate. Reads were trimmed using TrimGalore 0.6.7 (github.com/FelixKrueger/TrimGalore) with no quality filter and a length filter of 30. Reads were subsequently aligned to the African common hippo reference genome (GenBank: GCA_023065835.1) using BWA-mem 0.7.17. Reads with a mapping quality below 30,

unmapped and, in the case of paired-end sequencing data, unpaired reads were removed with samtools 1.9. Duplicate reads were marked using MarkDuplicates in picard 2.26.11 (http://broadinstitute.github.io/picard/). After filtering, a total of 1'845'041'892, 499'769'574, 720'280'245 and 30'909'422 sequencing reads were retained for ACH1, ACH2, WPH1 and NK37, respectively, which resulted in respective average coverages of 39.7x, 75.7x, 42.7x and 0.476x. As expected for ancient samples sequenced with single strand libraries, the sequencing data NK37 showed clear patterns of post-mortem damage at both the 5' and 3' end (Figure S1). Heterozygosity (θ) was estimated from genotype likelihoods as outlined in Kousathanas et al. ¹⁰⁸ and implemented in ATLAS¹⁰⁹ pipeline (bitbucket.org/wegmannlab/atlas, commit f1ec7fd), using the functions estimateErrors and theta. In brief, this approach first estimates post-mortem damage patterns and sequencing error rates, which are then used to calculate accurate genotype likelihoods. From these, heterozygosity is subsequently inferred as the rate θ = 2T μ under Felsenstein's substitution model¹¹⁰. Error rates were modeled using the following covariates: quality score, position in thread, mapping quality, fragment length and context (i.e. the previous base sequenced). The model was inferred from all sequence data on the X chromosome assuming no heterozygosity as all samples were males. θ was then inferred in 458 5Mb windows along all autosomes. Given their high sequencing quality, diversity estimation in modern samples (ACH1, ACH2, WPH1) were not affected by post-mortem damage and X chromosome-based recalibration (Figure S1). In contrast, they strongly reduce diversity overestimation in NK37 (Figure S1). To confirm the accuracy of the inferred post-mortem damage patterns and sequencing error rates, and consequently of diversity estimates, θ was also inferred from sequencing data down-sampled to 0.5x,0.2x, 0.1x and 0.05x using the task theta with the option -probs. Under accurate estimates of post-mortem damage patterns and sequencing error rates, the diversity estimates are expected to be rather insensitive to the sequencing depth. In case of over- or underestimated sequencing errors, however, the diversity is expected to be under or overestimated, respectively, at low depth. Inferred values of θ indeed were robust against down-sampling (at least as low as 0.1x; Figure 3), suggesting that post-mortem damage patterns are sequencing error rates, and that consequently genetic diversity was inferred with high accuracy.

626 627

628

599

600

601

602

603

604

605

606

607

608

609

610

611

612

613

614

615

616

617

618

619

620

621

622

623

624

625

Supplemental information

- 629 **Document S1: Figures S1-S3**
- 630 Table S1. Statistics and results of paleogenetic analysis, related to Figures 1, 3 and S1-S2 and STAR
- 631 Methods
- Table S2. Results of radiocarbon dating and amino acid racemization chronology, related to Figures
- 633 2 and S3 and STAR Methods

634

References

637

- 638 1. Koenigswald, W. von (1988). Paläoklimatische Aussage letztinterglazialer Säugetiere aus der
- 639 nördlichen Oberrheinebene. In Zur Paläoklimatologie des letzten Interglazials im Nordteil der
- Oberrheinebene, W. von Koenigswald, ed. (Gustav Fischer Verlag), pp. 205–314.
- 641 2. Koenigswald, W. von (1991). Exoten in der Großsäuger-Fauna des letzten Interglazials von
- 642 Mitteleuropa. E&G Quaternary Science Journal 41, 70–84.
- 643 3. Koenigswald, W. von (2007). Mammalian faunas from the interglacial periods in Central Europe
- and their stratigraphic correlation. Developments in Quaternary Sciences 7, 445–454.
- 645 4. Kolfschoten, T. van (2002). The Eemian mammal fauna of the northwestern and central
- 646 European continent. Le Dernier Interglaciaire et les occupations humaines du Paléolithique moyen.
- 647 CERP, Lille, 21–30.
- 648 5. Koenigswald, W. von (2003). Mode and causes for the Pleistocene turnovers in the mammalian
- fauna of Central Europe. Deinsea 10, 305–312.
- 650 6. Förster, M.W., and Sirocko, F. (2016). The ELSA tephra stack: Volcanic activity in the Eifel during
- the last 500,000 years. Global and Planetary Change 142, 100–107.
- 652 7. Faure, M. (1985). Les hippopotames quaternaires non-insulaires d'Europe occidentale.
- Nouvelles Archives du Muséum d'Histoire Naturelle de Lyon 23, 13–79.
- 654 8. Pushkina, D. (2007). The Pleistocene easternmost distribution in Eurasia of the species
- associated with the Eemian *Palaeoloxodon antiquus* assemblage. Mammalian Review 37, 224–245.
- 656 9. Mazza, P. (1991). Interrelations between Pleistocene hippopotami of Europe and Africa.
- 657 Bollettino della Società Paleontologica Italiana 30, 153–186.
- 658 10. Mecozzi, B., Iannucci, A., Mancini, M., Tentori, D., Cavasinni, C., Conti, J., Messina, M.Y., Sarra,
- A., and Sardella, R. (2023). Reinforcing the idea of an early dispersal of *Hippopotamus amphibius* in
- 660 Europe: Restoration and multidisciplinary study of the skull from the Middle Pleistocene of Cava
- Montanari (Rome, central Italy). PLoS One 18, e0293405.
- 662 11. Gabriel, G., Ellwanger, D., Hoselmann, C., Weidenfeller, M., Wielandt-Schuster, U., Heidelberg
- 663 Basin Project Team, and others (2013). The Heidelberg Basin, Upper Rhine Graben (Germany): a unique
- archive of Quaternary sediments in Central Europe. Quaternary International 292, 43–58.
- 665 12. Koenigswald, W. von (2011). Discontinuities in the faunal assemblages and early human
- 666 populations of Central and Western Europe during the Middle and Late Pleistocene. In Continuity and
- discontinuity in the peopling of Europe: one hundred fifty years of Neanderthal study, Condemi S and
- 668 Weniger GC, eds. (Springer), pp. 101–112.
- 669 13. Koenigswald, W. von, and Heinrich, W.-D. (1999). Mittelpleistozäne Säugetierfaunen aus
- 670 Mitteleuropa-der Versuch einer biostratigraphischen Zuordnung. Kaupia 9, e112.
- 671 14. Schweiss, D. (1988). Jungpleistozäne Sedimentation in der nördlichen Oberrheinebene. Zur
- 672 Paläoklimatologie des letzten Interglazials im Nordteil der Oberrheinebene. Paläoklimaforschung 4,
- 673 19-78.
- 674 15. Stoffel, C., Dufresnes, C., Okello, J.B.A., Noirard, C., Joly, P., Nyakaana, S., Muwanika, V.B.,
- 675 Alcala, N., Vuilleumier, S., and Siegismund, H.R. (2015). Genetic consequences of population

- 676 expansions and contractions in the common hippopotamus (Hippopotamus amphibius) since the Late
- 677 Pleistocene. Molecular Ecology 24, 2507–2520.
- 678 16. Lindauer, S., Knipper, C., Döppes, D., Knapp, H., Friedrich, R., and Rosendahl, W. (2022).
- 679 Investigating cave bear remains an overview on methods with focus on radiocarbon dating and stable
- isotopes. e- Research Reports of Museum Burg Golling 2, 1–20.
- 681 17. Mol, D., de Vos, J., and van der Plicht, J. (2007). The presence and extinction of Elephas
- antiquus Falconer and Cautley, 1847, in Europe. Quaternary International 169, 149–153.
- 683 18. Stuart, A.J. (2005). The extinction of woolly mammoth (Mammuthus primigenius) and straight-
- tusked elephant (*Palaeoloxodon antiquus*) in Europe. Quaternary International 126, 171–177.
- 685 19. Svensson, A., Andersen, K.K., Bigler, M., Clausen, H.B., Dahl-Jensen, D., Davies, S.M., Johnsen,
- 686 S.J., Muscheler, R., Rasmussen, S.O., Röthlisberger, R., et al. (2006). The Greenland ice core chronology
- 687 2005, 15–42 ka. Part 2: comparison to other records. Quaternary Science Review 25, 3258–3267.
- 688 20. Malmierca-Vallet, I., and Sime, L.C. (2023). Dansgaard-Oeschger events in climate models:
- review and baseline Marine Isotope Stage 3 (MIS3) protocol. Climate of the Past 19, 915–942.
- 690 21. Rasmussen, S.O., Bigler, M., Blockley, S.P., Blunier, T., Buchardt, S.L., Clausen, H.B., Cvijanovic,
- 691 I., Dahl-Jensen, D., Johnsen, S.J., Fischer, H., et al. (2014). A stratigraphic framework for abrupt climatic
- changes during the Last Glacial period based on three synchronized Greenland ice-core records:
- refining and extending the INTIMATE event stratigraphy. Quaternary Science Review 106, 14–28.
- 694 22. Behre, K.-E. (1989). Biostratigraphy of the last glacial period in Europe. Quaternary Science
- 695 Review 8, 25–44.
- 696 23. Preusser, F. (2004). Towards a chronology of the Late Pleistocene in the northern Alpine
- 697 Foreland. Boreas 33, 195–210.
- 698 24. Döppes, D., Rabeder, G., and Stiller, M. (2011). Was the Middle Würmian in the High Alps
- 699 warmer than today? Quaternary International 245, 193–200.
- 700 25. Sirocko, F., Martíinez-Garcíia, A., Mudelsee, M., Albert, J., Britzius, S., Christl, M., Diehl, D.,
- 701 Diensberg, B., Friedrich, R., Fuhrmann, F., et al. (2021). Muted multidecadal climate variability in
- 702 central Europe during cold stadial periods. Nature Geoscience 14, 651–658.
- 703 26. Sirocko, F., Albert, J., Britzius, S., Dreher, F., Martíinez-García, A., Dosseto, A., Burger, J.,
- 704 Terberger, T., and Haug, G. (2022). Thresholds for the presence of glacial megafauna in central Europe
- during the last 60,000 years. Scientific Reports 12, 20055.
- 706 27. Britzius, S., and Sirocko, F. (2023). Vegetation Dynamics and Megaherbivore Presence of MIS 3
- 707 Stadials and Interstadials 10–8 Obtained from a Sediment Core from Auel Infilled Maar, Eifel, Germany.
- 708 Quaternary 6, 44.
- 709 28. Britzius, S., Dreher, F., Maisel, P., and Sirocko, F. (2024). Vegetation patterns during the last
- 710 132,000 years: a synthesis from twelve Eifel Maar sediment cores (Germany): the ELSA-23-Pollen-
- 711 Stack. Quaternary 7, 8.
- 712 29. Menzies, J., and Ellwanger, D. (2015). Climate and paleo-environmental change within the
- 713 Mannheim Formation near Heidelberg, Upper Rhine Valley, Germany: a case study based upon
- 714 microsedimentological analyses. Quaternary International 386, 137–147.

- 715 30. Moine, O., Antoine, P., Hatté, C., Landais, A., Mathieu, J., Prud'homme, C., and Rousseau, D.-
- 716 D. (2017). The impact of Last Glacial climate variability in west-European loess revealed by radiocarbon
- 717 dating of fossil earthworm granules. Proceedings of the National Academy of Sciences 114, 6209–6214.
- 718 31. Antoine, P., Rousseau, D.-D., Moine, O., Kunesch, S., Hatté, C., Lang, A., Tissoux, H., and Zöller,
- 719 L. (2009). Rapid and cyclic aeolian deposition during the Last Glacial in European loess: a high-
- 720 resolution record from Nussloch, Germany. Quaternary Science Review 28, 2955–2973.
- 721 32. Fischer, P., Jöris, O., Fitzsimmons, K.E., Vinnepand, M., Prud'Homme, C., Schulte, P., Hatté, C.,
- Hambach, U., Lindauer, S., Zeeden, C., et al. (2021). Millennial-scale terrestrial ecosystem responses to
- 723 Upper Pleistocene climatic changes: 4D-reconstruction of the Schwalbenberg Loess-Palaeosol-
- 724 Sequence (Middle Rhine Valley, Germany). Catena 196, 104913.
- 725 33. Münzing, K., and Stobler, I. (1992). Pleistozäne Mollusken aus Bohrungen im nördlichen
- 726 Kaiserstuhlvorland. Jahreshefte des Geologischen Landesamtes in Baden-Württemberg 34, 395–399.
- 727 34. Ritchie, A.M., Lo, N., and Ho, S.Y.W. (2017). The impact of the tree prior on molecular dating
- of data sets containing a mixture of inter-and intraspecies sampling. Systematic Biology 66, 413–425.
- 729 35. Okello, J.B.A., Nyakaana, S., Masembe, C., Siegismund, H.R., and Arctander, P. (2005).
- 730 Mitochondrial DNA variation of the common hippopotamus: evidence for a recent population
- 731 expansion. Heredity 95, 206–215.
- 732 36. Stoffel, C., Dufresnes, C., Okello, J.B.A., Noirard, C., Joly, P., Nyakaana, S., Muwanika, V.B.,
- 733 Alcala, N., Vuilleumier, S., Siegismund, H.R., et al. (2015). Genetic consequences of population
- 734 expansions and contractions in the common hippopotamus (*Hippopotamus amphibius*) since the Late
- 735 Pleistocene. Molecular Ecology 24, 2507–2520.
- 736 37. Rabinovich, R., and Biton, R. (2011). The Early-Middle Pleistocene faunal assemblages of
- 737 Gesher Benot Ya 'aqov: inter-site variability. Journal of Human Evolution 60, 357–374.
- 738 38. Klein, R.G., Avery, G., Cruz-Uribe, K., and Steele, T.E. (2007). The mammalian fauna associated
- 739 with an archaic hominin skullcap and later Acheulean artifacts at Elandsfontein, Western Cape
- 740 Province, South Africa. Journal of Human Evolution 52, 164–186.
- 741 39. Hooijer, D.A., and Singer, R. (1961). The fossil hippopotamus from Hopefield, South Africa.
- 742 Zoologische Mededelingen 37, 157–165.
- 743 40. Martino, R., and Pandolfi, L. (2022). The Quaternary Hippopotamus records from Italy.
- 744 Historical Biology 34, 1146–1156.
- 745 41. Pandolfi, L., and Petronio, C. (2015). A brief review of the occurrences of Pleistocene
- 746 *Hippopotamus* (Mammalia, Hippopotamidae) in Italy. Geologia Croatica 68, 313–319.
- 747 42. Schreve, D.C. (2009). A new record of Pleistocene hippopotamus from River Severn terrace
- 748 deposits, Gloucester, UK—palaeoenvironmental setting and stratigraphical significance. Proceedings
- 749 of the Geologists' Association 120, 58–64.
- 750 43. Fidalgo, D., Madurell-Malapeira, J., Martino, R., Pandolfi, L., and Rosas, A. (2024). An updated
- 751 review of the Quaternary hippopotamus fossil records from the Iberian Peninsula. Quaternary 7, 4.
- 752 44. Rey-Iglesia, A., Lister, A.M., Campos, P.F., Brace, S., Mattiangeli, V., Daly, K.G., Teasdale, M.D.,
- 753 Bradley, D.G., Barnes, I., and Hansen, A.J. (2021). Exploring the phylogeography and population
- dynamics of the giant deer (*Megaloceros giganteus*) using Late Quaternary mitogenomes. Proceedings
- 755 of the Royal Society B 288, 20201864.

- 756 45. Lord, E., Dussex, N., Kierczak, M., Díiez-del-Molino, D., Ryder, O.A., Stanton, D.W.G., Gilbert,
- 757 M.T.P., Sanchez-Barreiro, F., Zhang, G., Sinding, M.-H.S., et al. (2020). Pre-extinction demographic
- 758 stability and genomic signatures of adaptation in the woolly rhinoceros. Current Biology 30, 3871-
- 759 3879.
- 760 46. Chang, D., Knapp, M., Enk, J., Lippold, S., Kircher, M., Lister, A., MacPhee, R.D.E., Widga, C.,
- 761 Czechowski, P., Sommer, R., et al. (2017). The evolutionary and phylogeographic history of woolly
- mammoths: a comprehensive mitogenomic analysis. Scienific Reports 7, 44585.
- Hofreiter, M., Serre, D., Rohland, N., Rabeder, G., Nagel, D., Conard, N., Münzel, S., and Pääbo,
- 764 S. (2004). Lack of phylogeography in European mammals before the last glaciation. Proceedings of the
- 765 National Academy of Sciences 101, 12963–12968.
- 766 48. Mallon, D., Wrightman, C., De Ornellas, P., Collen, B., and Ransom, C. (2011). Conservation
- strategy for the pygmy hippopotamus (IUCN Species Survival Commission).
- 768 49. Spielman, D., Brook, B.W., and Frankham, R. (2004). Most species are not driven to extinction
- 769 before genetic factors impact them. Proceedings of the National Academy of Sciences 101, 15261-
- 770 15264.
- 771 50. O'Ryan, C., Harley, E.H., Bruford, M.W., Beaumont, M., Wayne, R.K., and Cherry, M.I. (1998).
- 772 Microsatellite analysis of genetic diversity in fragmented South African buffalo populations. Animal
- 773 Conservation 1, 85–94.
- 774 51. Vrijenhoek, R.C. (1994). Genetic diversity and fitness in small populations. In Conservation
- 775 genetics (Springer), pp. 37–53.
- 776 52. Kahlke, R. (1994). Die Entstehungs-, Entwicklungs-und Verbreitungsgeschichte-des
- 777 oberpleistozänen *Mammuthus-Coelodonta-*Faunenkomplexes-in Eurasien (Großsäuger).
- Abhandlungen der Senckenbergischen Naturforschenden Gesellschaft 546, 1–64.
- 779 53. Mol, D., and Bakker, R. (2022). Quaternary terrestrial megafaunal remains and their localities
- in the southern bight of the North Sea between the British Isles and the Netherlands: an overview.
- 781 Staringia 17, 88–127.
- 782 54. Döppes, D., and Rosendahl, W. (2018). The Reiss-Engelhorn-Museen. In Paleontological
- 783 Collections of Germany, Austria and Switzerland: The History of Life of Fossil Organisms at Museums
- and Universities, L.A. Beck and U. Joger, eds. (Springer), pp. 411–418.
- 785 55. Ziegler, P.A. (1994). Cenozoic rift system of western and central Europe: an overview.
- Netherlands Journal of Geosciences–Geologie en Mijnbouw 73, 99–127.
- 787 56. Ellwanger, D., Gabriel, G., Simon, T., Wielandt-Schuster, U., Greiling, R.O., Hagedorn, E.-M.,
- Hahne, J., and Heinz, J. (2008). Long sequence of Quaternary rocks in the Heidelberg Basin depocentre.
- 789 E&G Quaternary Science Journal 57, 316–337.
- 790 57. Gabriel, G., Ellwanger, D., Hoselmann, C., and Weidenfeller, M. eds. (2009). The Heidelberg
- 791 Basin Drilling Project 3/4 (E&G Quaternary Science Journal).
- 792 58. Hoselmann, C. (2009). The Pliocene and Pleistocene fluvial evolution in the northern Upper
- 793 Rhine Graben based on results of the research borehole at Viernheim (Hessen, Germany). E&G
- 794 Quaternary Science Journal 57, 286–314.

- 795 59. Preusser, F., Büschelberger, M., Kemna, H.A., Miocic, J., Mueller, D., and May, J.-H. (2021).
- 796 Exploring possible links between Quaternary aggradation in the Upper Rhine Graben and the glaciation
- 797 history of northern Switzerland. International Journal of Earth Sciences 110, 1827–1846.
- 798 60. Scheidt, S., Hambach, U., and Rolf, C. (2015). A consistent magnetic polarity stratigraphy of late
- 799 Neogene to Quaternary fluvial sediments from the Heidelberg Basin (Germany): A new time frame for
- the Plio-Pleistocene palaeoclimatic evolution of the Rhine Basin. Global and Planetary Change 127,
- 801 103-116.
- 802 61. Knipping, M. (2008). Early and Middle Pleistocene pollen assemblages of deep core drillings in
- 803 the northern Upper Rhine Graben, Germany. Netherlands Journal of Geosciences-Geologie en
- 804 Mijnbouw 87, 51–65.
- 805 62. Gegg, L., Jacob, L., Moine, O., Nelson, E., Penkman, K.E.H., Schwahn, F., Stojakowits, P., White,
- 806 D., Wielandt-Schuster, U., and Preusser, F. (2024). Climatic and tectonic controls on deposition in the
- Heidelberg Basin, Upper Rhine Graben, Germany. Quaternary Science Review 345, 109018.
- 808 63. Lauer, T., Frechen, M., Hoselmann, C., and Tsukamoto, S. (2010). Fluvial aggradation phases in
- 809 the Upper Rhine Graben—new insights by quartz OSL dating. Proceedings of the Geologists'
- 810 Association 121, 154–161.
- 811 64. Lauer, T., Krbetschek, M., Frechen, M., Tsukamoto, S., Hoselmann, C., and Weidenfeller, M.
- 812 (2011). Infrared radiofluorescence (IR-RF) dating of middle Pleistocene fluvial archives of the
- Heidelberg Basin (Southwest Germany). Geochronometria 38, 23–33.
- 814 65. Kromer, B., Lindauer, S., Synal, H.-A., and Wacker, L. (2013). MAMS-a new AMS facility at the
- 815 Curt-Engelhorn-Centre for Achaeometry, Mannheim, Germany. Nuclear Instruments and Methods in
- Physics Research Section B 294, 11–13.
- 817 66. Brown, T.A., Nelson, D.E., Vogel, J.S., and Southon, J.R. (1988). Improved collagen extraction
- 818 by modified Longin method. Radiocarbon 30, 171–177.
- 819 67. Lindauer, S., Tomasto-Cagigao, E., and Fehren-Schmitz, L. (2015). The skeletons of Lauricocha:
- 820 New data on old bones. Journal of Archaeological Science: Reports 4, 387–394.
- 821 68. Reimer, P.J., Austin, W.E.N., Bard, E., Bayliss, A., Blackwell, P.G., Ramsey, C.B., Butzin, M.,
- 822 Cheng, H., Edwards, R.L., Friedrich, M., et al. (2020). The IntCal20 Northern Hemisphere radiocarbon
- age calibration curve (0–55 cal kBP). Radiocarbon 62, 725–757.
- 824 69. Bronk Ramsey, C. (2001). Development of the radiocarbon calibration program. Radiocarbon
- 825 43, 355–363.
- 826 70. Hajdas, I., Guidobaldi, G., Haghipour, N., and Wyss, K. (2024). Sample selection,
- 827 characterization and choice of treatment for accurate radiocarbon Analysis—Insights from the Eth
- 828 laboratory. Radiocarbon 66, 1152–1165.
- 71. Dickinson, M.R., Lister, A.M., and Penkman, K.E.H. (2019). A new method for enamel amino
- acid racemization dating: a closed system approach. Quaternary Geochronology 50, 29–46.
- 831 72. Dickinson, M.R., Scott, K., Adams, N.F., Lister, A.M., and Penkman, K.E.H. (2024). Amino acid
- dating of Pleistocene mammalian enamel from the River Thames terrace sequence: a multi-taxon
- approach. Quaternary Geochronology 82, 101543.
- 834 73. Gibbard, P.L., and Stuart, A.J. (1975). Flora and vertebrate fauna of the Barrington Beds.
- 835 Geological Magazine 112, 493–501.

- 836 74. Gao, C., and Boreham, S. (2011). Ipswichian (Eemian) floodplain deposits and terrace
- stratigraphy in the lower Great Ouse and Cam valleys, southern England, UK. Boreas 40, 303–319.
- 838 75. Lewis, S.G., Ashton, N.M., and Jacobi, R. (2011). Testing human presence during the Last
- 839 Interglacial (MIS 5e): a review of the British evidence. In The Ancient Human Occupation of Britain, N.
- Ashton, S. Lewis, and C. Stringer, eds. (Elsevier), pp. 125–164.
- Penkman, K.E.H., Preece, R.C., Bridgland, D.R., Keen, D.H., Meijer, T., Parfitt, S.A., White, T.S.,
- and Collins, M.J. (2011). A chronological framework for the British Quaternary based on Bithynia
- 843 opercula. Nature 476, 446–449.
- 844 77. Ashton, N., and Lewis, S. (2002). Deserted Britain: declining populations in the British late
- Middle Pleistocene. Antiquity 76, 388–396.
- 846 78. Sutcliffe, A.J. (1995). Insularity of the British Isles 250 000–30 000 years ago: the mammalian,
- including human, evidence. In Island Britain: A Quaternary Perspective, Geological Society of London
- 848 Special Publication, R. C. Preece, ed. (The Geological Society of London), pp. 127–140.
- Nelson, E., Penkman, K.E.H., White, D., Wheeler, L., Wedel, J., Hoselmann, C., Heggemann, H.,
- and Rähle, W. (2025). An aminostratigraphy of the northern Upper Rhine Graben, Germany. Journal of
- 851 Quaternary Science.

- 853 80. Dabney, J., Knapp, M., Glocke, I., Gansauge, M.-T., Weihmann, A., Nickel, B., Valdiosera, C.,
- 854 García, N., Pääbo, S., and Arsuaga, J.-L. (2013). Complete mitochondrial genome sequence of a Middle
- 855 Pleistocene cave bear reconstructed from ultrashort DNA fragments. Proceedings of the National
- 856 Academy of Sciences 110, 15758–15763.
- 857 81. Meyer, M., Kircher, M., Gansauge, M.-T., Li, H., Racimo, F., Mallick, S., Schraiber, J.G., Jay, F.,
- Prüfer, K., De Filippo, C., et al. (2012). A high-coverage genome sequence from an archaic Denisovan
- 859 individual. Science 338, 222–226.
- 860 82. Gansauge, M.-T., Gerber, T., Glocke, I., Korlević, P., Lippik, L., Nagel, S., Riehl, L.M., Schmidt, A.,
- and Meyer, M. (2017). Single-stranded DNA library preparation from highly degraded DNA using T4
- DNA ligase. Nucleic Acids Research 45, e79–e79.
- 863 83. Paijmans, J.L.A., Baleka, S., Henneberger, K., Taron, U.H., Trinks, A., Westbury, M. V, and
- 864 Barlow, A. (2017). Sequencing single-stranded libraries on the Illumina NextSeq 500 platform. arXiv
- 865 preprint arXiv:1711.11004.
- 866 84. Taron, U.H., Paijmans, J.L.A., Barlow, A., Preick, M., Iyengar, A., Drăgușin, V., Vasile, Ștefan,
- Marciszak, A., Robl\'\ičková, M., and Hofreiter, M. (2021). Ancient DNA from the Asiatic wild dog (Cuon
- alpinus) from Europe. Genes 12, 144.
- 869 85. Martin, M. (2011). Cutadapt removes adapter sequences from high-throughput sequencing
- 870 reads. EMBnet. journal 17, 10–12.
- 871 86. Magoč, T., and Salzberg, S.L. (2011). FLASH: fast length adjustment of short reads to improve
- genome assemblies. Bioinformatics 27, 2957–2963.
- 873 87. Li, H., and Durbin, R. (2009). Fast and accurate short read alignment with Burrows-Wheeler
- transform. Bioinformatics 25, 1754–1760.

- 875 88. Li, H., Handsaker, B., Wysoker, A., Fennell, T., Ruan, J., Homer, N., Marth, G., Abecasis, G.,
- 876 Durbin, R., and Subgroup, 1000 Genome Project Data Processing (2009). The sequence alignment/map
- format and SAMtools. bioinformatics 25, 2078–2079.
- 878 89. Li, H. (2013). Aligning sequence reads, clone sequences and assembly contigs with BWA-MEM.
- 879 arXiv:1303.3997.
- 880 90. Korneliussen, T.S., Albrechtsen, A., and Nielsen, R. (2014). ANGSD: analysis of next generation
- 881 sequencing data. BMC Bioinformatics 15, 1–13.
- 882 91. Hempel, E., Bibi, F., Faith, J.T., Koepfli, K.-P., Klittich, A.M., Duchêne, D.A., Brink, J.S., Kalthoff,
- 883 D.C., Dalén, L., Hofreiter, M., et al. (2022). Blue turns to gray: paleogenomic insights into the
- 884 evolutionary history and extinction of the blue antelope (*Hippotragus leucophaeus*). Molecular Biology
- and Evolution 39, msac241.
- 886 92. Schliep, K.P. (2011). phangorn: phylogenetic analysis in R. Bioinformatics 27, 592–593.
- 887 93. Minh, B.Q., Schmidt, H.A., Chernomor, O., Schrempf, D., Woodhams, M.D., Von Haeseler, A.,
- and Lanfear, R. (2020). IQ-TREE 2: new models and efficient methods for phylogenetic inference in the
- genomic era. Molecular Biology and Evolution 37, 1530–1534.
- 890 94. van der Valk, T., Pečnerová, P., Díez-del-Molino, D., Bergström, A., Oppenheimer, J., Hartmann,
- 891 S., Xenikoudakis, G., Thomas, J.A., Dehasque, M., and Sağlıcan, E. (2021). Million-year-old DNA sheds
- light on the genomic history of mammoths. Nature 591, 265–269.
- 893 95. Jónsson, H., Ginolhac, A., Schubert, M., Johnson, P.L.F., and Orlando, L. (2013). mapDamage2.
- 0: fast approximate Bayesian estimates of ancient DNA damage parameters. Bioinformatics 29, 1682–
- 895 1684.
- 896 96. Larsson, A. (2014). AliView: a fast and lightweight alignment viewer and editor for large
- 897 datasets. Bioinformatics 30, 3276–3278.
- 898 97. Dierckxsens, N., Mardulyn, P., and Smits, G. (2017). NOVOPlasty: de novo assembly of
- 899 organelle genomes from whole genome data. Nucleic Acids Research 45, e18-e18.
- 900 98. Katoh, K., and Standley, D.M. (2013). MAFFT multiple sequence alignment software version 7:
- 901 improvements in performance and usability. Molecular Biology and Evolution 30, 772–780.
- 902 99. Kalyaanamoorthy, S., Minh, B.Q., Wong, T.K.F., von Haeseler, A., and Jermiin, L.S. (2017).
- 903 ModelFinder: fast model selection for accurate phylogenetic estimates. Nature Methods 14, 587–589.
- 904 https://doi.org/10.1038/nmeth.4285.
- 905 100. Hoang, D.T., Chernomor, O., Von Haeseler, A., Minh, B.Q., and Vinh, L.S. (2018). UFBoot2:
- 906 improving the ultrafast bootstrap approximation. Molecular Biology and Evolution 35, 518–522.
- 907 101. Shimodaira, H. (2002). An approximately unbiased test of phylogenetic tree selection.
- 908 Systematic Biology 51, 492–508.
- 909 102. Leigh, J.W., and Bryant, D. (2015). POPART: full-feature software for haplotype network
- 910 construction. Methods in Ecology and Evolution 6, 1110–1116.
- 911 103. Bouckaert, R., Heled, J., Kühnert, D., Vaughan, T., Wu, C.-H., Xie, D., Suchard, M.A., Rambaut,
- 912 A., and Drummond, A.J. (2014). BEAST 2: a software platform for Bayesian evolutionary analysis. PLoS
- 913 Computational Biology 10, e1003537.

- 914 104. Psonis, N., Vassou, D., Nicolaou, L., Roussiakis, S., Iliopoulos, G., Poulakakis, N., and
- 915 Sfenthourakis, S. (2022). Mitochondrial sequences of the extinct Cypriot pygmy hippopotamus confirm
- 916 its phylogenetic placement. Zoological Journal of the Linnean Society 196, 979–989.
- 917 105. Boisserie, J.-R., Suwa, G., Asfaw, B., Lihoreau, F., Bernor, R.L., Katoh, S., and Beyene, Y. (2017).
- 918 Basal hippopotamines from the upper Miocene of Chorora, Ethiopia. Journal of Vertebrate
- 919 Paleontology 37, e1297718.
- 920 106. Rambaut, A., Drummond, A.J., Xie, D., Baele, G., and Suchard, M.A. (2018). Posterior
- 921 summarization in Bayesian phylogenetics using Tracer 1.7. Systematic Biology 67, 901–904.
- 922 107. Marchi, N., Winkelbach, L., Schulz, I., Brami, M., Hofmanová, Z., Blöcher, J., Reyna-Blanco, C.S.,
- Diekmann, Y., Thiéry, A., Kapopoulou, A., et al. (2022). The genomic origins of the world's first farmers.
- 924 Cell 185, 1842–1859.
- 925 108. Kousathanas, A., Leuenberger, C., Link, V., Sell, C., Burger, J., and Wegmann, D. (2017). Inferring
- heterozygosity from ancient and low coverage genomes. Genetics 205, 317–332.
- 927 109. Link, V., Kousathanas, A., Veeramah, K., Sell, C., Scheu, A., and Wegmann, D. (2017). ATLAS:
- analysis tools for low-depth and ancient samples. bioRxiv. https://doi.org/10.1101/105346.
- 929 110. Felsenstein, J. (1981). Evolutionary trees from DNA sequences: a maximum likelihood
- 930 approach. Journal of Molecular Evolution 17, 368–376.